Condition for optimal preamplifier decoupling in one-turn single- and multi-gap shielded loop MRI detectors

Wang, Wenjun; Sanchez, Juan Diego; Zhurbenko, Vitaliy; Ardenkjær-Larsen, Jan Henrik

Published in:
2022 IEEE Ukrainian Microwave Week (UkrMW)

Link to article, DOI:
10.1109/UkrMW58013.2022.10037007

Publication date:
2023

Document Version
Peer reviewed version

Condition for optimal preamplifier decoupling in one-turn single- and multi-gap shielded loop MRI detectors

Wenjun Wang
National Space Institute
Technical University of Denmark
2800 Kongens Lyngby, Denmark

Juan Diego Sánchez-Heredia
Department of Health Technology
Technical University of Denmark
2800 Kongens Lyngby, Denmark

Vitaliy Zhurbenko
National Space Institute
Technical University of Denmark
2800 Kongens Lyngby, Denmark
vizh@dtu.dk

Jan Henrik Ardenkjær-Larsen
Department of Health Technology
Technical University of Denmark
2800 Kongens Lyngby, Denmark

***Abstract*—Shielded loops have recently attracted keen interest in the design of Magnetic Resonance Imaging (MRI) detector arrays. To prevent unwanted detuning of array elements, preamplifier decoupling is used. So far, the decoupling circuit design was based on intuitive approach of minimizing impedance presented to the terminals of the loop. The approach leads to decent but not optimal results. In this paper a systematic analytical method is used to derive the exact condition for maximum decoupling of shielded loops in array. The condition describes precisely what impedance should be presented to the terminals of the loop for best decoupling. It is shown that the method is valid for single- and multi-gap shielded loops with and without integrated reactive components across the gap. The presented results are useful in the design of MRI receive arrays of shielded loop coils with optimal decoupling.**

Keywords—high impedance coil, magnetic resonance, radio frequency coil, shielded loop.

I. Introduction

Shielded loop antennae are widely used for sensing magnetic field [1]–[3]. These antennae can be made in various forms like multi-turn multi-gap [4], [5] and Möbius loops [6]. In 2018, Zhang et al. introduced shielded loops into magnetic resonance imaging (MRI), referring to them as "high-impedance coils" [7]. Since then, they attracted great interest in MRI community due to the fact that they also exhibit low noise correlation when assembled in arrays [7]–[9].

Simple loop antennae, named "coils" by the MRI community, are extensively used as receiving antennae in MRI. When put in arrays, the spatial proximity of loops introduces mutual inductance and thus de-tuning, complicating antenna matching and signal processing. To make loop antennae less sensitive to the interaction, a common technique is to overlap loops so that the mutual inductance becomes very low [10]. Another method is to present high impedance to loop coils to suppress coil current [10], which is named "preamplifier decoupling". Back when Zhang et al. introduced shielded loops into MRI, they recognized that low impedance needs to be presented to high-impedance coils for good preamplifier decoupling, i.e., good current suppression on the outer shield [7]. However, this was largely empirical. A dispute was raised by Mollaei et al. [11] that a pure inductance, instead of short circuit, should be presented to a one-turn one-gap shielded loop for preamplifier decoupling. We have proposed a preamplifier decoupling condition [12] assuming maximum current on the loop port, claiming that an impedance with a low real part and an imaginary part, that cancels the loop reactance, should be presented to a shielded loop, but no rigorous argument exists therein.

In this paper, it is shown that, for one-turn multi-gap (1TMG) shielded loops, to maximize suppression of current on the shield when the low-noise amplifier (LNA) impedance Z_a and matching/decoupling network's output impedance $Z_{out,M}$ are predetermined (by noise and impedance properties of LNA), as shown in Fig. 1, *impedance* $Z_{in,M}$ *of low resistance and reactance that cancels loop reactance should be presented to the shielded loop*. This statement holds whether tuning components are put across gaps or not [13]. *For a 1T1G shielded loop without tuning components*, $Z_{in,M}$ *resembles a low-loss inductor whose inductance equals the inductance of the outer shield at the resonance frequency*.

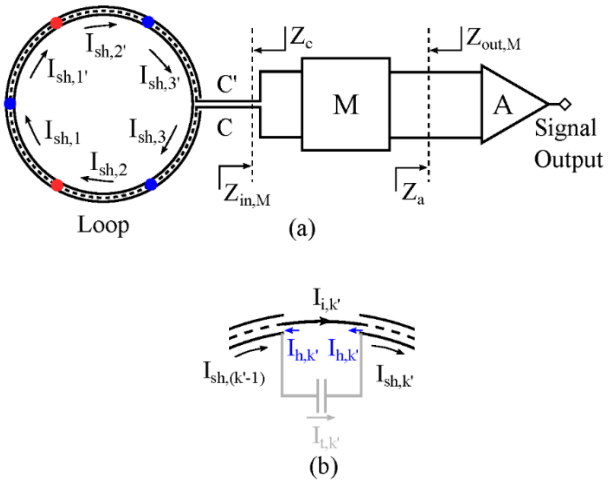

Fig. 1. (a) A 1TMG shielded loop connected to a matching network M, which is further connected to an amplifier. Here a 1T3G shielded loop is drawn for demonstration. (b) The current flow is shown across the gap. The tuning component is optional and drawn in grey.

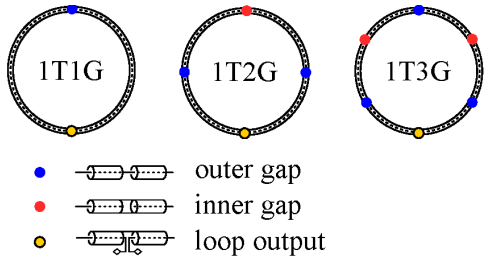

Fig. 2. Examples of 1TMG shielded loops.

II. Derivation of Optimal Decoupling Condition

A. Setup and assumptions

The setup of a shielded loop is shown in Fig. 1(a). The shielded loop reacts to external magnetic field, which induces voltage on the outer shield. We assume that the outer shield is thick enough so that electromagnetic field does not penetrate into the shield's inner surface, a condition generally satisfied in practice. The induced voltage can be represented by voltage sources distributed along the outer shield [14], [15]. The voltage further generates current on outer shields of sections of the shielded loop $I_{\mathrm{sh},1}$, $I_{\mathrm{sh},2}$… The 1TMG shielded loop has N gaps. For $N = 1,2,3$, the shielded loops are tailored as shown in Fig. 2. The loop output terminal CC' is terminated by a balanced matching network M followed by a balanced amplifier A. The shielded loop presents impedance Z_{c} to the matching network M, and the matching network M presents impedance $Z_{\mathrm{in,M}}$ to the shielded loop. The matching network M presents impedance $Z_{\mathrm{out,M}}$ to the amplifier A, and the amplifier A presents impedance Z_{a} to the matching network. The matching network can be arbitrarily constructed or adjusted, but its output impedance $Z_{\mathrm{out,M}}$ is predetermined (and often is equal to the optimal noise impedance of the implemented LNA).

In addition, the following are assumed:

(i) The surface current distribution on each section of the outer shield of the shielded loop is sufficiently constant;
(ii) The shielded loop resonates when the matching network M is disconnected. Resonance in this case assumes maximum current on the outer shield at the desired frequency ω_{r};
(iii) All transmission line sections are lossless and operate in TEM mode;
(iv) The preamplifier has $\Re Z_{\mathrm{a}} > 0$. The matching network is lossless and has $\Re Z_{\mathrm{in,\,m}} > 0$.

Please be aware that, although assumption (ii) is used as a condition of resonance in this paper, other definitions of resonance can be found in literature, like $\Im Z_{\mathrm{c}} = 0$ [4].

In the following subsections, without further clarification, Z stands for impedance, R stands for resistance and X stands for reactance. Corresponding quantities are marked by subscripts. For example, R_{a} means $\Re Z_{\mathrm{a}}$, X_{a} means $\Im Z_{\mathrm{a}}$.

B. Two-port network analysis

First, we notice the current distribution on the outer shield is sufficiently constant along the shielded loop in Fig. 1(a):

$$\begin{aligned} &I_{\mathrm{sh},1'} = I_{\mathrm{sh},2'} = \cdots = I_{\mathrm{sh},N'} \\ &= I_{\mathrm{sh},1} = I_{\mathrm{sh},2} = \cdots = I_{\mathrm{sh},N}\,. \end{aligned} \tag{1}$$

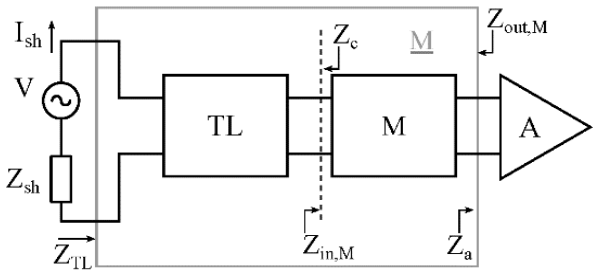

Fig. 3. The equivalent two-port representation of the multi-port problem with respect to gaps on a shielded loop. The extended matching network $\underline{M}$ consists of M and TL.

To see this, take any gap of the outer shield, say an outer gap k', as shown in Fig. 1(b).

i. If there is no tuning component across the gap, $I_{\mathrm{sh},(k'-1)}$ flows into the shield's inner surface. Since the transmission line operates in TEM mode (assumption (ii)), we have $I_{\mathrm{sh},(k'-1)} = I_{\mathrm{h},k'} = I_{\mathrm{i},k'} = I_{\mathrm{sh},k'}$.
ii. If there is a tuning component across the gap—typically an inductor or a capacitor—we have $I_{\mathrm{sh},(k'-1)} = I_{\mathrm{t},k'} - I_{\mathrm{h},k'}$. Since $I_{\mathrm{t},k'} = I_{\mathrm{h},k'} + I_{\mathrm{sh},k'}$, we have $I_{\mathrm{sh},(k'-1)} = I_{\mathrm{sh},k'}$.

Therefore, we conclude that, whether a tuning component is present across the gap of outer shield, the current flows on the outer shields across the gap are equal. The current flows on the outer shields across a gap of inner pin can be shown equal in a similar way. Applying the reasoning to all gaps leads to (1).

Since the current on all sections of the outer shield is equal, we denote the current as I_{sh}. We then infer that, for each section, denoting the impedance of outer shields as $Z_{\mathrm{sh},k}$, we have

$$\begin{aligned} V_{\mathrm{sh},k} &= I_{\mathrm{sh}} Z_{\mathrm{sh},k} \\ \Rightarrow V = \sum_{k,k'} V_{\mathrm{sh},k} &= I_{\mathrm{sh}} \sum_{k,k'} Z_{\mathrm{sh},k} = I_{\mathrm{sh}} Z_{\mathrm{sh}}\,. \end{aligned} \tag{2}$$

The multi-port excitation problem is essentially reduced to a two-port problem as shown in Fig. 3, in which transmission line sections and tuning components are gathered in a block TL.

C. Statements

Having shown that the problem under investigation is essentially a two-port problem, we are ready to prove our central statement.

We notice that, as the matching network and all transmission line sections are lossless (assumptions (iii), (iv)), the matching network M and the intermediary network TL can be regarded as an extended lossless matching network $\underline{M}$. Since the output impedance of the matching network $Z_{\mathrm{out,M}}$, and the preamplifier impedance Z_{a} are predetermined, to achieve $\min I_{\mathrm{sh}}$ or $\max I_{\mathrm{sh}}$ on the outer shield, according to [12], there must be $\Im[Z_{\mathrm{TL}} + Z_{\mathrm{sh}}] = 0$ if $|Z_{\mathrm{TL}}| < \infty$, which is ensured by assumption (iv). This can be summarized in Statement 1.

Statement 1. *If the matching network's output impedance $Z_{out,m}$ is fixed, to achieve the minimum or maximum current on the outer shield, the outer shield's reactance must be cancelled by transmission line sections.*

To show what $Z_{\mathrm{in,M}}$ must be presented to the matching network, laborious circuit simulation seems inevitable for 1T1G, 1T2G, 1T3G… and for a myriad combinations of tuning components. Here, however, Statement 2 reveals an underlying consistency across all cases of 1TMG loops.

Statement 2. *At the resonant frequency ω_r, let a lossless, reciprocal two-port network TL have $X_{TL}|_\infty + X_{sh} = 0$, where $X_{TL}|_\infty$ is the input reactance when M is disconnected from the network. If $X_c + X_{in,M} = 0$, then*

$$Z_{TL} = \frac{R_c R_{sh}}{R_{in,M}} - jX_{sh}.$$

Conversely, if $X_{TL} + X_{sh} = 0$, then $X_c + X_{in,M} = 0$.

Proof. The impedance matrix of a lossless, reciprocal two-port network can be written as [16]

$$\mathbf{Z} = \mathrm{j}\begin{bmatrix} X_{11} & X_{\varnothing} \\ X_{\varnothing} & X_{22} \end{bmatrix} \tag{3}$$

where X_{11}, $X_{\varnothing}$, X_{22} are real numbers. By definition of an impedance matrix, the input impedance when the load is disconnected from the network is $\mathrm{j}X_{11}$, so $X_{11} = X_{\mathrm{TL}}|_\infty = -X_{\mathrm{sh}}$. The output impedance of the network is

$$\begin{aligned} Z_{\mathrm{c}} &= \mathrm{j}X_{22} + \frac{X_{\varnothing}^2}{\mathrm{j}X_{11} + R_{\mathrm{sh}} + \mathrm{j}X_{\mathrm{sh}}} \\ &= \mathrm{j}X_{22} + \frac{X_{\varnothing}^2}{R_{\mathrm{sh}}}. \end{aligned} \tag{4}$$

Therefore $X_{\mathrm{c}} = \Im Z_{\mathrm{c}} = X_{22}$. Using $X_{\mathrm{c}} + X_{\mathrm{in,M}} = 0$, the input impedance becomes

$$\begin{aligned} Z_{\mathrm{TL}} &= \mathrm{j}X_{11} + \frac{X_{\varnothing}^2}{\mathrm{j}X_{22} + R_{\mathrm{in,M}} + \mathrm{j}X_{\mathrm{in,M}}} \\ &= \mathrm{j}X_{11} + \frac{X_{\varnothing}^2}{R_{\mathrm{in,M}}}. \end{aligned} \tag{5}$$

Using $R_{\mathrm{c}} = \Re Z_{\mathrm{c}} = X_{\varnothing}^2/R_{\mathrm{sh}}$, and $X_{11} = -X_{\mathrm{sh}}$, we arrive at $Z_{\mathrm{TL}} = \left(R_{\mathrm{c}}R_{\mathrm{sh}}/R_{\mathrm{in,M}}\right) - \mathrm{j}X_{\mathrm{sh}}$.

To show the reverse statement, apply $X_{11} = -X_{\mathrm{sh}}$ to the left and middle sides of (4), and we infer $X_{22} + X_{\mathrm{in,M}} = 0$. Apply $X_{11} = -X_{\mathrm{sh}}$ and $X_{22} + X_{\mathrm{in,M}} = 0$ to the left and middle sides of (5), and the reverse statement is proven. □

From assumption (ii), when the matching network M is disconnected, I_{sh} reaches its maximum. According to Statement 1, we must have $X_{\mathrm{TL}}|_\infty + X_{\mathrm{sh}} = 0$. Again, according to Statement 1, to have the minimum I_{sh}, we must have $X_{\mathrm{TL}} + X_{\mathrm{sh}} = 0$, which, according to Statement 2, implies $X_{\mathrm{c}} + X_{\mathrm{in,M}} = 0$. This again means $R_{\mathrm{TL}} = R_{\mathrm{c}}R_{\mathrm{sh}}/R_{\mathrm{in,M}}$. To achieve the minimum I_{sh}, R_{TL} has to be as high as possible, which is achieved by low $R_{\mathrm{in,M}}$. If we define "maximum preamplifier decoupling" as "minimum I_{sh}", which is employed in [12], we conclude Statement 3.

Statement 3. *For a self-resonant 1TMG shield loop, when the matching network has fixed output impedance $Z_{out,M}$, to achieve the maximum preamplifier decoupling on the outer shield, the matching network must exhibit to the shielded loop low input resistance $R_{in,M}$ and input reactance that cancels the loop reactance, i.e., $X_{in,M} + X_c = 0$.*

This statement is what we seek. It applies to all cases of self-resonant 1TMG shielded loops regardless of the ways gaps are cut and the presence of tuning components across gaps.

D. Special case: 1T1G shielded loops

We now apply Statement 3 to a one-turn one-gap (1T1G) shielded loop. Mollaei et al. [11] claim a pure inductance should be presented to a 1T1G shielded loop without tuning components for maximum preamplifier decoupling; we show this is a corollary of Statement 3. In all following discussions, we focus on differential mode operation.

The equivalent circuit schematic of a 1T1G shielded loop is shown in Fig. 4(a) [14], [15]. Voltage V is induced on the outer shield of the shielded loop. The impedance on the outer shield can be modelled by an inductor L_{sh} in series with a resistor R_{sh}. A tuning capacitor C_{t} strides across the gap. For a loop of small electric size, the reactance of the outer shield can be approximated by $X_{\mathrm{sh}}(\omega) = \omega L_{\mathrm{sh}}$, where [17]

$$L_{\mathrm{sh}} \approx \mu_0 b\left(\ln\frac{8b}{a} - 2\right), \tag{6}$$

μ_0 is the permeability in vacuum, b is the loop radius, a is the coaxial cable's radius. Under differential mode operation, the voltage along the horizontal centre line is 0, giving half the equivalent circuit shown in Fig. 4(b), where $\tilde{C} = 2C$, $\tilde{L} = L/2$, $\tilde{R} = R/2$, $\tilde{Z} = Z/2$, $\tilde{V} = V/2$.

From assumption (ii), the shielded loop resonates when the matching network M is disconnected, which can be represented by disconnecting $\tilde{Z}_{\mathrm{in,M}}$ on Fig. 4. The input admittance of an open-circuited transmission line is [18]

$$\tilde{Y}_{\mathrm{TL}}\big|_\infty = \mathrm{j}Y_0\tan(\beta\tilde{l}), \tag{7}$$

where $Y_0 = 1/Z_0 = 1/50$ S is the characteristic admittance, $\beta = \omega/v$ is the wave number, $\tilde{l}$ is half the loop circumference. At the resonant frequency ω_{r}, according to Statement 1, there must be $\tilde{X}_{\mathrm{TL}}(\omega_{\mathrm{r}})\big|_\infty + \tilde{X}_{\mathrm{sh}}(\omega_{\mathrm{r}}) = 0$, so we have

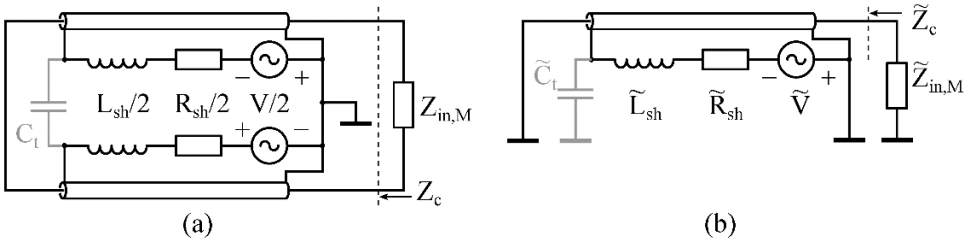

Fig. 4. (a) The circuit schematic of a 1T1G shielded loop. C_{t} is an optional tuning capacitor. (b) Half the circuit under differential operation. Component values are $\tilde{C} = 2C$, $\tilde{L} = L/2$, $\tilde{R} = R/2$, $\tilde{Z} = Z/2$, $\tilde{V} = V/2$.

$$\frac{1}{\tilde{Y}_{\mathrm{TL}}\big|_{\infty}+\mathrm{j}\omega_{\mathrm{r}}\tilde{C}_{\mathrm{t}}}+\mathrm{j}\omega_{\mathrm{r}}\tilde{L}_{\mathrm{sh}}=0$$
$$\Rightarrow\quad Y_0\tan\left(\beta_{\mathrm{r}}\tilde{l}\right)=\frac{1}{\omega_{\mathrm{r}}\tilde{L}_{\mathrm{sh}}}-\omega_{\mathrm{r}}\tilde{C}_{\mathrm{t}}. \tag{8}$$

The impedance of the shielded loop is

$$\tilde{Z}_{\mathrm{c}}(\omega)=Z_0\frac{\tilde{Z}_{\mathrm{st}}+\mathrm{j}Z_0\tan\left(\beta\tilde{l}\right)}{Z_0+\mathrm{j}\tilde{Z}_{\mathrm{st}}\tan\left(\beta\tilde{l}\right)}, \tag{9}$$

where

$$\tilde{Z}_{\mathrm{st}}=\left(\mathrm{j}\omega\tilde{C}_{\mathrm{t}}+\frac{1}{\tilde{R}_{\mathrm{sh}}+\mathrm{j}\omega\tilde{L}_{\mathrm{sh}}}\right)^{-1}. \tag{10}$$

We then have

$$\tilde{Z}_{\mathrm{c}}(\omega_{\mathrm{r}})=\frac{\left(\omega_{\mathrm{r}}\tilde{L}_{\mathrm{sh}}\right)^2}{\tilde{R}_{\mathrm{sh}}}\left(Z_0^2B_{\mathrm{st}}^2+1\right)-\mathrm{j}\omega_{\mathrm{r}}\tilde{L}_{\mathrm{sh}}\left(Z_0^2\omega_{\mathrm{r}}\tilde{C}_{\mathrm{t}}B_{\mathrm{st}}+1\right), \tag{11}$$

where

$$B_{\mathrm{st}}=\omega_{\mathrm{r}}\tilde{C}_{\mathrm{t}}-\frac{1}{\omega_{\mathrm{r}}\tilde{L}_{\mathrm{sh}}}.$$

From Statement 3, we conclude that the matching network must have a low $\tilde{R}_{\mathrm{m}}$ and

$$\tilde{X}_{\mathrm{in,M}}(\omega_{\mathrm{r}})=-\Im\tilde{Z}_{\mathrm{c}}(\omega_{\mathrm{r}})=\omega_{\mathrm{r}}\tilde{L}_{\mathrm{sh}}\left(Z_0^2\omega_{\mathrm{r}}\tilde{C}_{\mathrm{t}}B_{\mathrm{st}}+1\right). \tag{12}$$

The sign of $\tilde{X}_{\mathrm{in,M}}$ is hard to determine since the term $\omega_{\mathrm{r}}\tilde{C}_{\mathrm{t}}-1/\left(\omega_{\mathrm{r}}\tilde{L}_{\mathrm{sh}}\right)<0$; otherwise, according to (8), $\tan\left(\beta_{\mathrm{r}}\tilde{l}\right)<0\Rightarrow\beta_{\mathrm{r}}\tilde{l}>\pi/2$, implying that the electric length of the transmission line section is not short, meaning that the current distribution on its outer shield is unlikely to be sufficiently constant, which violates assumption (i).

When the tuning component C_{t} is not present, $\tilde{C}_{\mathrm{t}}$ can be replaced by 0 in (11). The matching network M must still have low $\tilde{R}_{\mathrm{in,M}}$. Half of M's reactance is given by

$$\tilde{X}_{\mathrm{in,M}}(\omega_{\mathrm{r}})=-\lim_{\tilde{C}_{\mathrm{t}}\to 0}\Im\tilde{Z}_{\mathrm{c}}(\omega_{\mathrm{r}})=\omega_{\mathrm{r}}\tilde{L}_{\mathrm{sh}}. \tag{13}$$

Finally, using $R=2\tilde{R}$, $X=2\tilde{X}$, we conclude that the matching network M presents low $R_{\mathrm{in,M}}$ and $X_{\mathrm{in,M}}=\omega_{\mathrm{r}}L_{\mathrm{sh}}$. Therefore, the matching network M should appear like an inductor to the shielded loop, and the inductance equals the inductance of the outer shield.

Summarizing the reasoning above, we have Corollary 3.1.

Corollary 3.1 *For a 1T1G shielded loops, to reach the minimum current on the outer shield at the resonant frequency ω_r, when a tuning component across the gap is not present , the matching network should appear like a low-loss inductor to the shielded loop, of which the inductance equals the outer shield's inductance.*

Mollaei et al. have also concluded that the matching network should appear like an inductor to a 1T1G shielded loop [11] when a tuning component is not present. However, the procedure to derive the exact value of the inductance was not given.

III. Experimental Verification

To study the influence of the load impedance $Z_{\mathrm{in,M}}$ on the decoupling experimentally, a 8 cm diameter shielded loop was constructed using a standard RG316 coaxial cable. A double loop probe was positioned at a distance of 6 cm to measure the decoupling level, as illustrated in Fig. 5(a).

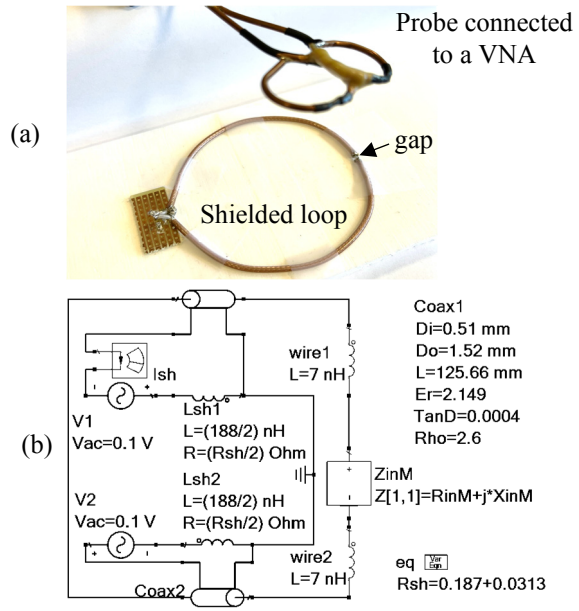

Fig. 5. (a) photograph of the measurement setup; (b) simulation setup.

The probe was connected to a VNA with output power 5 dBm and IF bandwidth 500 Hz.

The parameters of the corresponding circuit model are listed in Fig. 5(b) and obtained from eq. (6) and extracted from RG316 datasheet. Two 7 nH inductors are included to model 1 cm long connection wires at the loop terminal [19]. R_{sh} consists of resistive loss R_{ac} and radiation loss $R_r=376.7\times(\pi/6)\times(k_0b)^4=0.031\,3\ \Omega$ [17]. R_{ac} of the outer shield is assumed equal to the straight-wire R_{ac} with the current flowing uniformly on the wire surface and penetrating into the wire center by a skin depth δ: $R_{\mathrm{ac}}=l/[\pi\delta(2a-\delta)\sigma_0\sigma_r]=0.187\ \Omega$ [20], where l is the loop's perimeter, $\sigma_0=5.98\times10^7\ \mathrm{S/m}$ is copper's conductivity, and $\sigma_r=1/2.6$ is the conductivity relative to copper, extracted from RG316 loss (36 dB/100m). The relative permittivity of the cable dielectric was adjusted to reproduce the resonance frequency of the loop.

The simulated decoupling level versus $Z_{\mathrm{in,M}}$ at 133.5 MHz is shown in Fig. 6. It can be observed, that the best decoupling is achieved when $R_{\mathrm{in,M}}$ is minimized and $X_{\mathrm{in,M}}=158\ \Omega=\omega_r\times188\times10^{-9}\ \Omega$, which is predicted by eq. (13).

The measured versus simulated decoupling for three different circuit loads (open/short circuit, and an inductor) is shown in Fig. 7. The chosen inductor is a fixed value 150 nH Coilcraft 1812SMS-R15, which was the closest to the optimal inductance ($188\ \mathrm{nH}-2\times7\ \mathrm{nH}$) available for the experiment.

As can be concluded from the data in Fig. 7, a specially designed load at the terminals of the loop can increase decoupling beyond what can be achieved with a short circuit. The developed model in Fig. 4 and Fig. 5(b) predicts the behavior of the loop reasonably well. The measured coil Q factor is 250 while simulated 268.

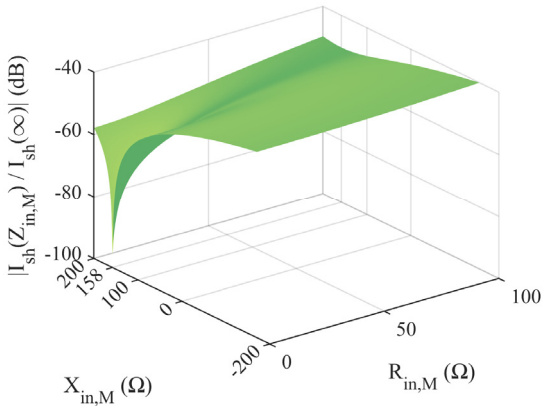

Fig. 6. Simulated decoupling level versus coil loading, $Z_{\mathrm{in,M}}$.

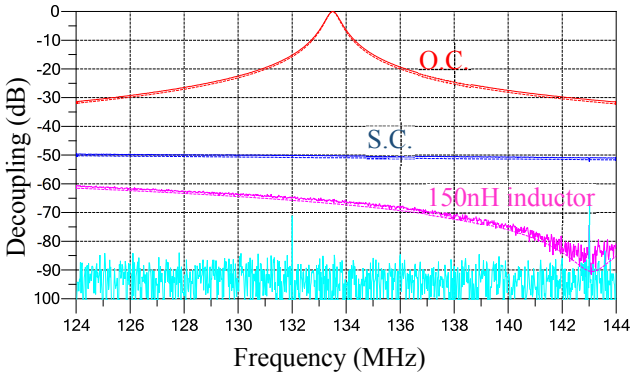

Fig. 7. —— measured $|S_{21}|$ when open circuited, $Z_{\mathrm{in,M}} = \infty$. – – – simulated I_{sh} when open circuited. —— measured $|S_{21}|$ when short circuited, $Z_{\mathrm{in,M}} = 0$. – – – simulated I_{sh} when short circuited. —— measured $|S_{21}|$ when loaded by 150 nH inductor, $Z_{\mathrm{in,M}} = \omega_r \times 150 \times 10^{-9}\ \Omega$. – – – simulated I_{sh} when loaded by 150nH inductor. The dashed lines overlap with solid lines very well, so that they might not be visible. All curves are normalized to the maximum at the resonance (when $Z_{\mathrm{in,M}} = \infty$). Measurements are also normalized by ω to remove frequency dependence of S-parameters. —— measurement noise floor.

IV. Discussion

The phrase "low resistance $R_{\mathrm{in,M}}$" in Statement 3 means a sufficiently small positive number. This meaning demonstrates itself in Statement 2 and assumption (iv). In practice, $R_{\mathrm{in,M}}$ usually lies in the range 10Ω–30Ω. "Low resistance" does not mean "zero resistance" in this article because of the following reasons:

- Resistance truly zero exists only in rare occasions in practice like superconduction.
- Zero resistance presented to a shielded loop can lead to LNA instability.
- How low $R_{\mathrm{in,M}}$ can reach is limited by LNA reflection coefficient, which is defined by Z_{a} and $Z_{\mathrm{out,M}}$ (refer to Fig. 1(a) for notation). If the matching network M is lossless, to achieve maximum preamplifier decoupling, according to [12], $R_{\mathrm{in,M}} = R_{\mathrm{c}}/\beta$, where $\beta = (1 + |\Gamma_{\mathrm{out}}|)/(1 - |\Gamma_{\mathrm{out}}|)$ is defined by the power reflection coefficient $\Gamma_{\mathrm{out}} = (Z_{\mathrm{out,M}} - Z_{\mathrm{a}}^*)/(Z_{\mathrm{out,M}} + Z_{\mathrm{a}})$.

Conclusion

To achieve maximum preamplifier decoupling in the shielded loop, it should be terminated with impedance $Z_{\mathrm{in,M}} = R_{\mathrm{in,M}} - \mathrm{j}X_{\mathrm{c}}$. The resistance $R_{\mathrm{in,M}}$ should be as low as possible; however, in practice, it is limited by the equivalent resistance of the loop as well as input impedance and optimal noise impedance of the implemented LNA. The decoupling reactance should equal $-\mathrm{j}X_{\mathrm{c}}$, i.e. cancel the loop reactance, no matter how many gaps are used.

Acknowledgment

The research is partly supported by Danish National Research Foundation under grant DNRF 124.

References

[1] J. D. Heebl, E. M. Thomas, R. P. Penno, and A. Grbic, "Comprehensive analysis and measurement of frequency-tuned and impedance-tuned wireless non-radiative power-transfer systems," *IEEE Antennas Propag. Mag.*, vol. 56, no. 4, pp. 44–60, Aug. 2014.

[2] J. D. Dyson, "Measurement of Near Fields of Antennas and Scatterers," *IEEE Trans. Antennas Propag.*, vol. 21, no. 4, pp. 446–460, 1973.

[3] D. I. Hoult, "The principle of reciprocity in signal strength calculations - A mathematical guide," *Concepts Magn. Reson.*, vol. 12, no. 4, pp. 173–187, Jan. 2000.

[4] L. Nohava *et al.*, "Flexible Multi-Turn Multi-Gap Coaxial RF Coils: Design Concept and Implementation for Magnetic Resonance Imaging at 3 and 7 Tesla," *IEEE Trans. Med. Imaging*, vol. 40, no. 4, pp. 1267–1278, Apr. 2021.

[5] J. E. Lindsay and K. Münter, "Distributed Parameter Analysis of Shielded Loops Used for Wide-Band H-Field Measurements," *IEEE Trans. Instrum. Meas.*, vol. 32, no. 1, pp. 241–244, 1983.

[6] O. Aluf, "Moebius loop antenna system stability analysis under parameters variation," in *2017 IEEE International Conference on Microwaves, Antennas, Communications and Electronic Systems, COMCAS 2017*, 2017, pp. 1–5.

[7] B. Zhang, D. K. Sodickson, and M. A. Cloos, "A high-impedance detector-array glove for magnetic resonance imaging of the hand," *Nat. Biomed. Eng.*, vol. 2, no. 8, pp. 570–577, Aug. 2018.

[8] T. Ruytenberg, A. Webb, and I. Zivkovic, "Shielded-coaxial-cable coils as receive and transceive array elements for 7T human MRI," *Magn. Reson. Med.*, vol. 83, no. 3, pp. 1135–1146, 2020.

[9] V. Zhurbenko, J. D. Sanchez-Heredia, W. Wang, and J. H. Ardenkjar-Larsen, "Flexible Self-Resonant Detector Coil for Magnetic Resonance Imaging of Carbon-13," in *2020 50th European Microwave Conference, EuMC 2020*, 2021, pp. 112–115.

[10] P. B. Roemer, W. A. Edelstein, C. E. Hayes, S. P. Souza, and O. M. Mueller, "The NMR phased array," *Magn. Reson. Med.*, vol. 16, no. 2, pp. 192–225, Nov. 1990.

[11] M. S. M. Mollaei, C. C. Van Leeuwen, A. J. E. Raaijmakers, and C. R. Simovski, "Analysis of High Impedance Coils Both in Transmission and Reception Regimes," *IEEE Access*, vol. 8, pp. 129754–129762, 2020.

[12] W. Wang, V. Zhurbenko, J. D. Sánchez-Heredia, J. H. Ardenkjær-Larsen, "Trade-off between preamplifier noise figure and decoupling in MRI detectors," *Magnetic Resonance in Medicine*, Published online, September 2022, pp. 1-13.

[13] V. Zhurbenko, J. D. Sánchez-Heredia, W. Wang, and J. H. Ardenkjær-Larsen, "Flexible Receive Array of Parallel-Resonance High-Impedance Coaxial Coils for ^{13}C Imaging," in *Proceedings of the Internation Society for Magnetic Resonance in Medicine 30*, 2022, p. 2261.

[14] M. D. Harpen, "The Theory of Shielded Loop Resonators," *Magn. Reson. Med.*, vol. 32, no. 6, pp. 785–788, 1994.

[15] L. L. Libby, "Special Aspects of Balanced Shielded Loops," *Proc. IRE*, vol. 34, no. 9, pp. 641–646, 1946.

[16] D. M. Pozar, "Chapter 4: Microwave Network Analysis," in *Microwave Engineering*, 4th ed., John Wiley & Sons, Inc., 2011, pp. 165–227.

[17] R. W. P. King, "The loop antenna for transmission and reception," in *Antenna Theory Part 1*, R. E. Collin and F. J. Zucker, Eds. McGraw-Hill, 1969, pp. 458–482.

[18] D. M. Pozar, "Chapter 2: Transmission Line Theory," in *Microwave Engineering*, 4th ed., Singapore: John Wiley & Sons, Inc., 2011, pp. 48–90.

[19] E.B. Rosa, "The self and mutual inductances of linear conductors". Bulletin of the Bureau of Standards. U.S. 1908. 4 (2): 301.

[20] P. R. Clayton "Analysis of Multiconductor Transmission Lines," 2nd Ed., 2008.